



HAL
open science

Large scale control of surface ozone by relative humidity observed during warm seasons in China

Mengying Li, Shaocai Yu, Xue Chen, Zhen Li, Yibo Zhang, Liqiang Wang, Weiping Liu, Pengfei Li, Eric Lichtfouse, Daniel Rosenfeld, et al.

► To cite this version:

Mengying Li, Shaocai Yu, Xue Chen, Zhen Li, Yibo Zhang, et al.. Large scale control of surface ozone by relative humidity observed during warm seasons in China. *Environmental Chemistry Letters*, 2021, 19, pp.3981 - 3989. 10.1007/s10311-021-01265-0 . hal-03409893

HAL Id: hal-03409893


<https://hal.science/hal-03409893>

Submitted on 30 Oct 2021

HAL is a multi-disciplinary open access archive for the deposit and dissemination of scientific research documents, whether they are published or not. The documents may come from teaching and research institutions in France or abroad, or from public or private research centers.

L'archive ouverte pluridisciplinaire **HAL**, est destinée au dépôt et à la diffusion de documents scientifiques de niveau recherche, publiés ou non, émanant des établissements d'enseignement et de recherche français ou étrangers, des laboratoires publics ou privés.

Large scale control of surface ozone by relative humidity observed during warm seasons in China

Mengying Li¹ · Shaocai Yu^{1,2}  · Xue Chen¹ · Zhen Li¹ · Yibo Zhang¹ · Liqiang Wang¹ · Weiping Liu¹ · Pengfei Li³ · Eric Lichtfouse⁴ · Daniel Rosenfeld⁵ · John H. Seinfeld²

Abstract

Rising air pollution by surface ozone (O_3) in China has induced extensive efforts to control ozone generation in major urban and industrial areas, yet mechanisms ruling the ozone production and loss are not well understood. In particular, ozone levels are strongly influenced by meteorological factors such as relative humidity, but this has been explored only in local situations, and the effect of relative humidity on ozone levels in warm seasons on a large scale in China is still unknown. Here we studied surface ozone, relative humidity, temperature, and other meteorological variables in 74 major cities in China during 2017–2018, focusing on the warm seasons in seven regions. Results show that ozone levels decrease with increasing relative humidity in all cities, with an average correlation coefficient of -0.58 , ranging from -0.17 in Zhangjiakou to -0.84 in Hengshui. At high relative humidity levels, above 75%, average ozone levels ranged from 44.6 to 122.5 $\mu\text{g m}^{-3}$, which is lower than Chinese quality threshold of hourly average ozone level of 200 $\mu\text{g m}^{-3}$. The decreases of ozone with relative humidity were more pronounced at high temperature, above 30 °C, than below 25 °C. The increases of ozone with temperature were more pronounced at low relative humidity, below 40%. Overall, our findings reveal that mechanisms ruling surface ozone levels are similar on a large scale. This is promising to design common methods of climate engineering to protect human health.

Keywords Ozone · Relative humidity · Temperature · Warm season · China

Introduction

Tropospheric ozone (O_3) is a major oxidant and greenhouse gas related partly to pollution. Ozone has negative impacts on human health, regional climates, agricultural yields, and forest productivity (Yu et al. 2006; Shao et al. 2006; Booker et al. 2009; Monks et al. 2015). Anthropogenic ozone is produced by photochemical reactions of nitrogen oxides (NO_x) and volatile organic compounds (VOCs) in the presence of sunlight (Seinfeld and Pandis 2016). High near-surface O_3 levels occur in many urban and industrial areas across China. The establishment of an atmospheric monitoring network since 2000 in China has allowed regular ozone monitoring. Hourly monitoring data in 74 major cities disclosed an increase of daily average maximum 8-h O_3 concentrations from about 69.5 ppbv in 2013 to 75 ppbv in 2015 (<http://www.mep.gov.cn>). Moreover, a 4.2% increase of mean O_3 concentrations in 336 prefecture-level cities was observed from 2015 to 2016 (Li et al. 2019). Recently, maximum 8-h O_3 concentrations

✉ Shaocai Yu
shaocaiyu@zju.edu.cn ; shaocaiyu@caltech.edu

✉ Pengfei Li
lpf_zju@163.com

¹ Key Laboratory of Environmental Remediation and Ecological Health, Ministry of Education, Research Center for Air Pollution and Health, College of Environmental and Resource Sciences, Zhejiang University, 310058 Hangzhou, Zhejiang, People's Republic of China

² Division of Chemistry and Chemical Engineering, California Institute of Technology, Pasadena, CA 91125, USA

³ College of Science and Technology, Hebei Agricultural University, Baoding, 071000 Hebei, People's Republic of China

⁴ Aix Marseille Univ, CNRS, INRAE, IRD, Europole Méditerranéenne de l'Arbois, Avenue Louis Philibert, 13545 Aix en Provence, France

⁵ Institute of Earth Sciences, Hebrew University of Jerusalem, Jerusalem, Israel

exceeding the China National Ambient Air Quality Standard of $160 \mu\text{g}/\text{m}^3$ (CNAAQ, GB3095-2012) have been observed in many regions in China, notably in Beijing-Tianjin-Hebei, Yangtze River Delta, and Pearl River delta (Wang et al. 2017).

Extensive efforts have been made to control surface ozone by reducing ozone precursors and controlling meteorological conditions (Ou et al. 2016; Wang et al. 2017; Chen et al. 2019a; Yang et al. 2019). Parameters ruling ozone levels include emissions, solar radiation, precipitation, temperature (T), relative humidity (RH), wind speed and direction, and cloud cover (Camalier et al. 2007; Davis et al. 2011; Reddy and Pfister 2016; Wang et al. 2017; Chen et al. 2019b; Li et al. 2019). Yu (2019) proposed a fog geoengineering method to increase atmospheric moisture and, in turn, abate near-surface O_3 levels. In this study, we focused on the effects of relative humidity on surface O_3 .

Relationships between O_3 and relative humidity have been investigated in modeling studies. For instance, maximum daily temperature and average relative humidity had the largest effects in 74 cities in the US according to a city-specific generalized linear model (Davis et al. 2011). The role of water vapor in the reduction of surface O_3 levels has also been demonstrated by simulations with Climate-chemistry models (CCMs) (Thompson et al. 1989; Johnson et al. 2001; Murazaki and Hess 2006; Doherty et al. 2013). A 19% increase of water vapor could lead to approximately 4–5% decrease of O_3 concentrations (Doherty et al. 2013). Similarly, the increasing relative humidity from 9 to 87% can reduce O_3 concentrations by 30% (Wang et al. 2016). The decrease of ozone with relative humidity has been explained by the following processes (Table S1):

- O_3 photolysis produces $\text{O}(^1\text{D})$. $\text{O}(^1\text{D})$ then reacts with a water molecule (H_2O) to generate two OH radicals, which favor ozone decomposition.
- Relative humidity favors heterogeneous reactions of O_3 with particles in aerosols (He et al. 2017a; b). For instance, humidity enhance ozone uptake by increasing aerosol size and decreasing aerosol viscosity (Han et al. 2019).
- Ozone decomposition is enhanced by heterogeneous bonding on aqueous aerosol surfaces (Kotelnikov and Stepanov 2019).
- Wet aerosols formed under high humidity reduce ultraviolet actinic flux and inhibit photochemical reaction rates (Deng et al. 2010; Liu et al. 2011).
- Elevated relative humidity decreases temperature by water evaporation (Olszyna et al. 1997).
- Relative humidity inhibits the chain length of hydroxyl radicals (OH and HO_2) and NO_2 , thus limiting O_3 generation (Reichert et al. 2003; Wang et al. 2016).

- High relative humidity promotes the reaction of gaseous N_2O_5 with aqueous NaCl particles, thus greatly reducing O_3 generation (Leu et al. 1995; Jia and Xu 2015).

Decreases of ozone with relative humidity have been reported in some regions and are commonly observed in summer seasons (Olszyna et al. 1997; Dueas et al. 2002; Elminir 2005; Camalier et al. 2007; Tu et al. 2007). A study in a coastal Spanish site showed that, together with temperature and wind speed, relative humidity was one of three dominant meteorological factors influencing ozone levels (Dueas et al. 2002). Pearson correlation and stepwise multiple regression analysis also showed negative correlations between ozone-RH (Manju et al. 2018). In Nanjing, a report shows a maximum O_3 level of 43.4 ppbv below 40% relative humidity, versus the lowest value of 10.9 ppbv above 80% RH (Tu et al. 2007). Relative humidity was also found as the strongest influencing factor in central and southern parts of eastern China (Han et al. 2020). Relative humidity appeared more important than radiation and temperature to assess the adverse effects of ozone on vegetation (Gong et al. 2021). Overall, previous investigations focused on local situations or several cities during the same time period. Therefore, here we present a study of ozone, relative humidity and temperature in different warm seasons at a large geographical scale in the major 74 cities in China.

Experimental

Monitoring data of O_3 and its precursors (NO_2 , CO) were collected from the website of the China National Environmental Monitoring Center (CNEMC, <http://www.mee.gov.cn/hjzl/dqbj/>). We focused on hourly O_3 concentrations measured at all monitoring sites in 74 major cities in China during 2017–2018. The monitoring data in each city consist of urban and background sites. The average O_3 concentrations at all sites in each separate city were used and regarded as the city-level O_3 values. Meteorological variable data on an hourly basis including temperature (T, °C), relative humidity (RH, %), precipitation (Prec, mm), and wind speed (WS, m/s) were provided by the China Meteorological Administration (<http://data.cma.cn/site/index.html>). Only hours with both valid O_3 and RH values were used for analysis. The data of leaf area indices (LAI) in the summer seasons and topography height (HGT_M) in China were derived from MODIS products (<https://modis.gsfc.nasa.gov/data/>).

Under the comprehensive consideration of the spatial patterns of O_3 and national administrative divisions in China, the following 74 cities were geographically grouped into seven representative divisions, namely Northeast China (Dalian, Haerbin, Shenyang, Changchun), North China (Baoding, Beijing, Cangzhou, Chengde, Handan, Hengshui,

Huhehaote, Langfang, Qinhuangdao, Shijiazhuang, Taiyuan, Tangshan, Tianjin, Xingtai, Zhangjiakou), Central China (Wuhan, Changsha, Zhengzhou), East China (Changzhou, Fuzhou, Hangzhou, Hefei, Huzhou, Huai'an, Jinan, Jiaxing, Jinhua, Lishui, Lianyungang, Nanchang, Nanjing, Nantong, Ningbo, Qingdao, Quzhou, Xiamen, Shanghai, Shaoxing, Suzhou, Taizhou, Taizhouj, Wenzhou, Wuxi, Suqian, Xuzhou, Yancheng, Yangzhou, Zhenjiang, Zhoushan), South China (Dongguan, Foshan, Guangzhou, Haikou, Huizhou, Jiangmen, Nanning, Shenzhen, Zhaoqing, Zhongshan, Zhuhai), Southwest China (Chengdu, Guiyang, Kunming, Chongqing, Lasa), and Northwest China (Lanzhou, Wulumuqi, Xian, Xining, Yinchuan), as seen in Fig. 1 and Table S2. Then, concentrations and meteorological data averaged across all cities located in each division were used. While conducting correlation analyses between O_3 and RH, we chose different study periods for the seven regions due to various warm seasons for each region, as based on monthly variations of temperature in Fig. 1. The national warm season typically spans April–September. But obviously the northern regions have lower temperatures than southern regions in May and September. So summer season

(June–August) is regarded as the warm season in northern areas in China. Since O_3 concentrations in South China typically peak in October (Lu et al. 2018), also shown in Fig. 1, the study period of cities in South China was expanded to October. Therefore, the final chosen study periods were June to August for Northeast China (NE), North China (NC), and Northwest China (NW), May to September for East China (EC), Central China (CC), and Southwest China (SW), May to October for South China (SC). Due to geographical proximity of Fuzhou and Xiamen cities to South China, time periods of these two cities were kept in correspondence with the cities in South China.

Results and discussion

Seasonal variations of O_3 , NO_2 and CO

Average levels of ozone (O_3), nitrogen dioxide (NO_2), carbon monoxide (CO), relative humidity (RH), and temperature (T) in various Chinese regions in 2018 are shown in Fig. 1, with warm seasons shadowed in orange. Results show

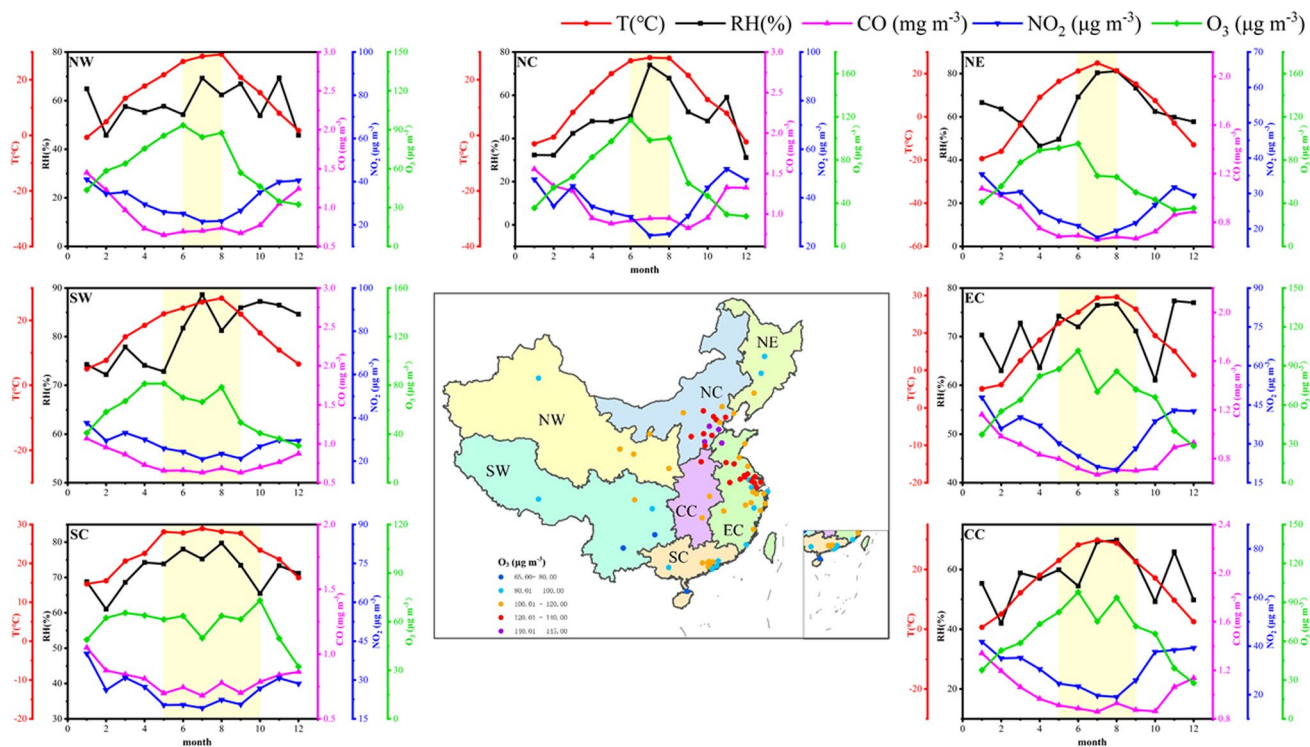


Fig. 1 Monthly variations of average concentrations of ozone (O_3), nitrogen dioxide (NO_2), and carbon monoxide (CO), and values of relative humidity (RH), and temperature (T) for Chinese areas in 2018. The orange-shaded areas denote chosen warm seasons: June to August for Northeast China (NE), North China (NC), and Northwest China (NW), May to September for East China (EC), Central China (CC), and Southwest China (SW), May to October for South China

(SC). Results show that six divisions displayed similar variation patterns of monthly average O_3 concentrations peaking in May or June, whereas South China reached seasonal peak in October when temperature was not maximum but RH was relatively low. Coincident high O_3 and low RH were generally observed in warm seasons for all the regions

that annual mean O₃ concentrations are heterogeneous in 74 cities, with values ranging from 65.8 μg m⁻³ in Haikou, Hainan province, to 143.8 μg m⁻³ in Cangzhou, Hebei province. The highest O₃ levels were mainly observed in North and East China and have been explained by greater emissions of ozone precursors in industrialized and urbanized regions. Indeed, in North China, power plants, coal combustion industries, and biomass burning sources produce more NO_x and VOCs emissions (Zhao et al. 2012; Chai et al. 2014). Higher NO₂ levels are also observed in cities having more vehicle emission sources (Wang et al. 2010a, b).

NO₂ and CO levels in all Chinese regions display similar variations, with maximum values in winter and late autumn, and minimum values in summer, late spring, and early autumn (Fig. 1). The low concentrations of these ozone precursors in warmer seasons can be attributed to active photochemistry and stronger vertical atmospheric mixing. Whereas the high levels in colder seasons may be a result of larger consumption of heating fuels, as well as weak solar radiation, low wind speed and mixing layer height, enhancing NO₂ and CO concentrations (Wang et al. 2010a; Tai et al. 2010).

Considerable seasonal variations of O₃ are observed in all Chinese regions, with high levels in summer, late spring, and early autumn, and low levels in winter (Fig. 1). Maximum ozone concentrations range from 73.1 μg m⁻³ in South China to 117.2 μg m⁻³ in North China. In general, monthly variations of O₃ can be explained by prevailing meteorological conditions and anthropogenic activities (Reddy and Pfister 2016). Peak values of ground-level O₃ tend to appear in the warm seasons with intense solar radiation, high temperature, stagnant high-pressure conditions, as observed previously (Ou et al. 2015; He et al. 2017b).

Nevertheless, we also observed inconsistent fluctuations in variation patterns. For example, monthly average O₃ concentrations displayed similar variations in six regions, peaking in May or June. Whereas South China displayed a seasonal ozone maximum in October when temperature was not maximum. This is likely due to the sharp decline of relative humidity from about 80% in August to 65% in October in South China. Similar findings have been shown in previous studies conducted in the Pearl River delta, with October being the most polluted month, different from other regions (Bell et al. 2005; Zanutti and Schwartz 2008). This phenomenon has also been attributed to the adverse effect of the Asian summer monsoon on O₃, with O₃ peaking before and after monsoon in the Yangtze River and Pearl River deltas (Lu et al. 2018; Han et al. 2020). Although higher temperature and longer sunshine duration in summer favors O₃ formation in South China, larger rainfall amounts in summer versus autumn can retard O₃ formation (Shao et al. 2009).

Overall, our findings show that high ground-level O₃ levels are generally accompanied by high temperature and

low relative humidity in all regions, whereas high NO₂ and CO concentrations appear under low temperature and high relative humidity. Since ozone peaked in warm seasons, we focused further research on warm seasons highlighted in orange in Fig. 1 to investigate relationships between ozone and relative humidity.

Correlation between ozone and relative humidity

Figure 2 displays correlations of O₃ versus relative humidity (RH) during the noontimes, 11:00–16:00 local time, during warm seasons of 2017 and 2018 in the major 74 cities in China. We excluded data of rainfall time to avoid the influence of precipitation scavenging. We selected noontimes when O₃ formation is higher due to stronger solar radiation, according to Monks et al. (2015). Moreover, data with low relative humidity, below 25% and temperature, below 15 °C, were excluded owing to little effect of low humidity and temperature on ozone. Correlation coefficient (R) and slope of linear regression equation (S) were used to represent the relationships. Unlike prior studies choosing the same time periods for all cities, here we focused on dates of warm seasons, which are different in the seven regions.

Results show an overall decrease of ozone levels with relative humidity in all major cities, with R coefficient ranging from -0.84 in Hengshui city to -0.17 in Zhangjiakou city, and slope values varying widely from -2.57 to -0.48 μg m⁻³/1%RH (Fig. 2). The average R coefficient for all cities is -0.58 ± 0.14. Moreover, hourly O₃ levels are strongly correlated with RH in most cities, with correlation coefficient below -0.5 in 57 cities. Also, we did not observe significant heterogeneity of correlations between Southern and Northern regions, contrary to previous research in China and abroad (Camalier et al. 2007; Kavassalis and Murphy 2017; Cheng et al. 2018). This discrepancy is explained by the fact that analyses of previous investigations compared data at the same dates for different locations, whereas here we used only data of warm seasons, which occur at different dates in different regions. For example, greater responses were observed in the southern versus northern areas in 39 US cities from May to September (Camalier et al. 2007). We also studied the effect of other meteorological factors on ozone variations (Fig. S5). Results show that the relative humidity effect is comparable to or even stronger than temperature, and far exceeds wind speed. In summary, we found that almost all cities have large negative correlations between RH and ozone in warm seasons.

The different influences of relative humidity on ozone observed in different cities and regions (Fig. 2) can be explained by chemical and meteorological drivers. For instance, low temperatures in Southwestern areas throughout the year reduces O₃ formation, while high radiation intensity

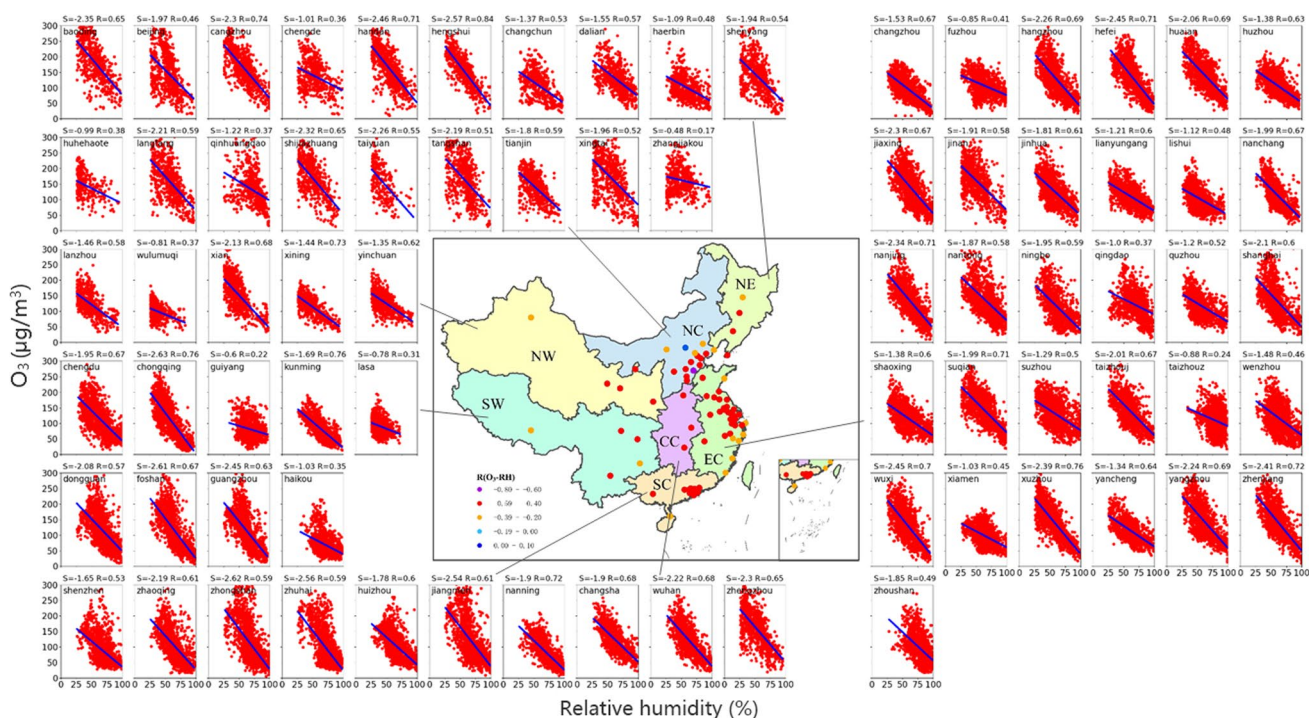


Fig. 2 Correlations between noontime O_3 and relative humidity (RH), 11:00–16:00 local time, excluding data points with precipitation and low RH and T ($RH \leq 25\%$, $T \leq 15^\circ C$) in warm seasons of 2017 and 2018 for the major 74 cities in China. Results without exclusion are

shown in figure S3. S denotes the slope of linear regression equation, and R denotes the correlation coefficient. Results show that almost all cities have strong correlations with average R value of -0.58 ± 0.14

and long solar duration favors O_3 production via enhancing the photolysis rates of NO_2 and reaction rates of NO and O_3 (Gaur et al. 2014). Also, long-range transport of pollutants from high emission areas to low emission regions can change precursor concentrations and further affect ozone-RH correlations.

Moreover, rising relative humidity increases the opening of tree stomata and, in turn, should induce the removal of ozone from air as a dry ozone sink (Kavassalis and Murphy 2017). To check this hypothesis, we tested the correlation of leaf area indices (LAI) with correlation coefficients of ozone and RH (Figure S1, Table S2). Our results indicate that the dry deposition of ozone in trees do not play a significant influence on the strong negative correlations between ozone and RH, in our conditions.

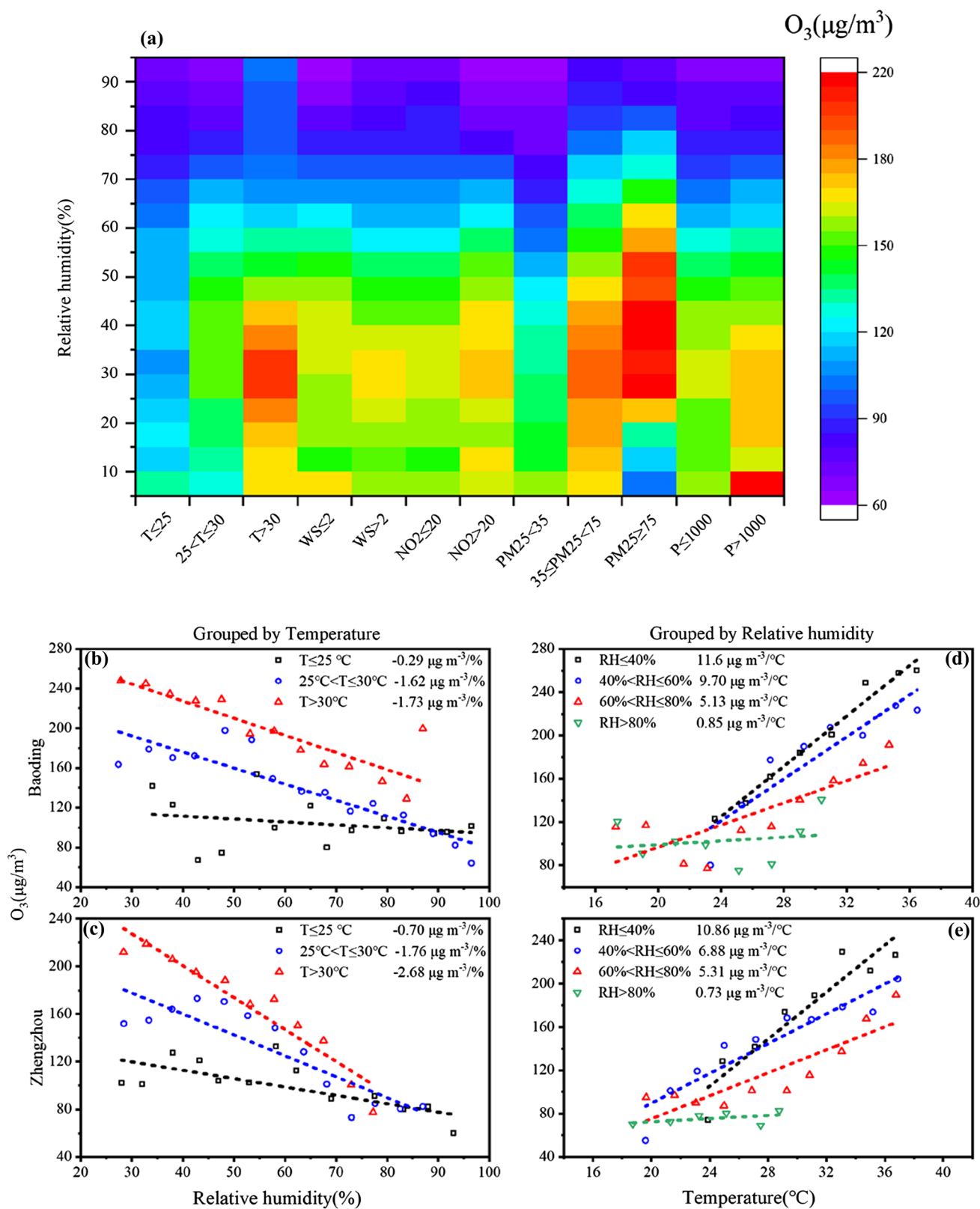
Table S3 shows the effects of high RH on O_3 decreases in all cities. For RH over 75%, the average O_3 concentrations varied from 44.6 to 122.5 $\mu g m^{-3}$ in these 74 cities, and the 90% percentile of hourly O_3 concentrations ranged from 75.6 to 168.7 $\mu g m^{-3}$, less than the quality standard of 200 $\mu g m^{-3}$. For O_3 concentrations exceeding 200 $\mu g m^{-3}$, the mean RH values ranged from 31 to 66%, with 90% percentile of hourly RH values varying from 36 to 81%. This shows that O_3 quality exceedance generally appeared under relatively low RH. In summary, our findings show that high

RH exerted great influence on O_3 attainment in warm seasons for all 74 cities.

Overall, our findings show that ozone levels decreases with relative humidity in all Chinese regions, that there is no significant differences between southern and northern regions if only warm seasons are considered, and that dry ozone deposition on trees is not a major influencing factor in our conditions. Further effects of meteorological factors are studied below.

Meteorological and chemical factors

We studied the effect of temperature, wind speed, surface pressure, NO_2 , and particulate matter ($PM_{2.5}$) concentrations, on ozone levels (Fig. 3a). Results show that O_3 concentrations display larger variation ranges with RH at high temperature, low wind speed, high pressure, and high NO_2 and $PM_{2.5}$ levels. Ozone can exceed 160 $\mu g m^{-3}$ below 40% low RH, with $PM_{2.5}$ over 35 $\mu g m^{-3}$ and NO_2 over 20 $\mu g m^{-3}$. This suggests the inducing effect of $PM_{2.5}$ and NO_2 on ozone, and implies that adverse health effects should be reduced by decreasing particulate matter and NO_2 emissions. On the other hand, when relative humidity exceeds 60%, O_3 concentrations are lower than 130 $\mu g m^{-3}$ under all conditions, except high $PM_{2.5}$ levels, above 75 $\mu g m^{-3}$.



This further demonstrates the important roles of high relative humidity for O_3 decreases and the need of joint control of PM $_{2.5}$ and O_3 .

We conducted a stratified analysis at four representative cities, Baoding in North China, Zhengzhou in Central China, Hangzhou in East China, and Chengdu in Southwest

Fig. 3 a The average O_3 concentrations for each relative humidity (RH) bin (5% intervals) in all the major cities grouped by temperature (T), wind speed (WS), pressure (P), NO_2 , and $PM_{2.5}$ concentrations (units: $^{\circ}C$, $m\ s^{-1}$, hPa, $\mu g\ m^{-3}$, $\mu g\ m^{-3}$, respectively). Scatter plots of O_3 against RH grouped by T during the noontime (11:00–16:00, local time) excluding precipitation in different warm seasons during 2017–2018 in **b** Baoding and **c** Zhengzhou. Points represent the average values of O_3 concentration versus RH for each RH bin (5% intervals). Scatter plots of O_3 against T grouped by RH during the same period as above in **d** Baoding and **e** Zhengzhou. Points represent the average values of O_3 concentrations versus T for each T bin ($2\ ^{\circ}C$ intervals). The slopes of linear regression equations are also provided in the plots ($\alpha < 0.05$). Results show that high temperature strengthened negative dependence of O_3 on RH, and high relative humidity not only lowered O_3 levels, but also weakened the positive effects of T on O_3

China to gain more knowledge on ozone response to relative humidity and temperature. These cities show high O_3 pollution, high negative correlations between O_3 and RH, with R below -0.5 , and a large distribution range of hourly temperature and relative humidity data. Correlations of O_3 versus RH at different temperature ranges are given in Figs. 3b, c, S4a, and S4b. Correlations of ozone versus temperature, grouped by relative humidity, are given in Figs. 3c, d, S4c, and S4d. Results show that the negative relationship between O_3 and RH became stronger under higher temperature in Baoding city, with an average decreasing rate of $-1.73\ \mu g\ m^{-3}/1\%RH$ above $30\ ^{\circ}C$ compared to $-0.29\ \mu g\ m^{-3}/1\%RH$ below $25^{\circ}C$. Similar variations were also found in Zhengzhou, Hangzhou and Chengdu with larger decreasing rates of O_3 as RH rose at higher temperature. This result indicates that the increase of relative humidity is effective to decrease O_3 concentrations at high temperature. The choice of the temperature range is therefore important to control O_3 levels in mitigation practices.

We also observed that stronger increasing rates of O_3 with temperature occurred under low relative humidity, below 40%, with 11.6, 10.86, 2.78, and $9.19\ \mu g\ m^{-3}/^{\circ}C$ in Baoding, Zhengzhou, Hangzhou, and Chengdu, respectively, much higher than 0.85, 0.73, 0.04, and $1.70\ \mu g\ m^{-3}/^{\circ}C$ in corresponding cities at high relative humidity, over 80%. Although under intermediate relative humidity, from 40 to 80%, increasing rates of O_3 were comparable to and even greater in Hangzhou and Chengdu than under low RH, the weakening effects of high RH, above 80%, on O_3 increase were evident in these two cities. This means that relative humidity can not only decrease ozone levels but also alleviate the positive effect of temperature on ozone generation. In summary, we found that high temperature strengthens the effects of relative humidity on ozone decrease, and that high relative humidity weakens the positive correlations between O_3 and temperature.

Conclusion

On the basis of observed pollutant concentrations and meteorological variables for the major 74 cities in China, we first studied seasonal variation patterns of O_3 , then conducted correlation analyses of O_3 and relative humidity during different warm seasons in 74 cities. Furthermore, the study discussed the effects of relative humidity and temperature on O_3 using stratified analyses aimed at four cities, i.e., Baoding, Zhengzhou, Hangzhou, Chengdu. O_3 levels displayed spatial differences among different regions, with higher levels mainly distributed in North China and East China. A considerable seasonal variation of O_3 was recorded in each region, showing peak values in warm seasons with intense solar radiation, stagnant high-pressure conditions. We found the overall negative correlations between O_3 and relative humidity in all cities, indicating the explanatory power of relative humidity to hourly variability of midday O_3 in the warm seasons. Also, the role of high relative humidity in O_3 attainment can be seen at all the cities. Then the stratified analyses show that high temperature can strengthen O_3 dependence on relative humidity, and high relative humidity can weaken the positive impacts of temperature on O_3 . Our results may have an implication for the great need of controlling the rising O_3 pollution, especially in regions having drier climate conditions with low relative humidity and soil water content.

Supplementary Information The online version contains supplementary material available at <https://doi.org/10.1007/s10311-021-01265-0>.

Acknowledgements This work was supported in part by the Department of Science and Technology of China (No. 2016YFC0202702, 2018YFC0213506, and 2018YFC0213503), National Research Program for Key Issues in Air Pollution Control in China (No. DQGG0107), and National Natural Science Foundation of China (No. 21577126 and 41561144004). Part of this work was also supported by the “Zhejiang 1000 Talent Plan” and Research Center for Air Pollution and Health in Zhejiang University. Pengfei Li is supported by National Natural Science Foundation of China (No. 22006030), Initiation Fund for Introducing Talents of Hebei Agricultural University (412201904), and Hebei Youth Top Fund (BJ2020032).

References

- Bell ML, Dominici F, Samet JM (2005) A meta-analysis of time-series studies of ozone and mortality with comparison to the national morbidity, mortality, and air pollution study. *Epidemiology* 16:436–445
- Booker F, Muntifering R, Mcgrath M et al (2009) The ozone component of global change: Potential effects on agricultural and horticultural plant yield, product quality and interactions with invasive species. *J Integr Plant Biol* 51:337–351
- Camalier L, Cox W, Dolwick P (2007) The effects of meteorology on ozone in urban areas and their use in assessing ozone trends.

- Atmos Environ 41:7127–7137. <https://doi.org/10.1016/j.atmosenv.2007.04.061>
- Chai F, Gao J, Chen Z et al (2014) Spatial and temporal variation of particulate matter and gaseous pollutants in 26 cities in China. *J Environ Sci (china)* 26:75–82. [https://doi.org/10.1016/S1001-0742\(13\)60383-6](https://doi.org/10.1016/S1001-0742(13)60383-6)
- Chen X, Situ S, Zhang Q et al (2019a) The synergetic control of NO₂ and O₃ concentrations in a manufacturing city of southern China. *Atmos Environ* 201:402–416. <https://doi.org/10.1016/j.atmosenv.2018.12.021>
- Chen Z, Zhuang Y, Xie X et al (2019b) Understanding long-term variations of meteorological influences on ground ozone concentrations in Beijing during 2006–2016. *Environ Pollut* 245:29–37. <https://doi.org/10.1016/j.envpol.2018.10.117>
- Cheng L, Wang S, Gong Z et al (2018) Regionalization based on spatial and seasonal variation in ground-level ozone concentrations across China. *J Environ Sci China* 67:179–190. <https://doi.org/10.1016/j.jes.2017.08.011>
- Davis J, Cox W, Reff A, Dolwick P (2011) A comparison of CMAQ-based and observation-based statistical models relating ozone to meteorological parameters. *Atmos Environ* 45:3481–3487. <https://doi.org/10.1016/j.atmosenv.2010.12.060>
- Deng J, Wang T, Liu L, Jiang F (2010) Modeling heterogeneous chemical processes on aerosol surface. *Particuology* 8:308–318. <https://doi.org/10.1016/j.partic.2009.12.003>
- Doherty RM, Wild O, Shindell DT et al (2013) Impacts of climate change on surface ozone and intercontinental ozone pollution: a multi-model study. *J Geophys Res Atmos* 118:3744–3763. <https://doi.org/10.1002/jgrd.502662013>
- Dueas C, Fernández MC, Caete S et al (2002) Assessment of ozone variations and meteorological effects in an urban area in the Mediterranean Coast. *Sci Total Environ* 299:97–113. [https://doi.org/10.1016/S0048-9697\(02\)00251-6](https://doi.org/10.1016/S0048-9697(02)00251-6)
- Elminir HK (2005) Dependence of urban air pollutants on meteorology. *Sci Total Environ* 350:225–237. <https://doi.org/10.1016/j.scitotenv.2005.01.043>
- Gaur A, Tripathi SN, Kanawade VP et al (2014) Four-year measurements of trace gases (SO₂, NO_x, CO, and O₃) at an urban location, Kanpur, in Northern India. *J Atmos Chem* 71:283–301. <https://doi.org/10.1007/s10874-014-9295-8>
- Gong C, Yue X, Liao H, Ma Y (2021) A humidity-based exposure index representing ozone damage effects on vegetation. *Environ Res Lett* 16:44030. <https://doi.org/10.1088/1748-9326/abecbb>
- Han H, Liu J, Shu L et al (2020) Local and synoptic meteorological influences on daily variability in summertime surface ozone in eastern China. *Atmos Chem Phys* 20:203–222. <https://doi.org/10.5194/acp-20-203-2020>
- Han Y, Gong Z, Ye J et al (2019) Quantifying the role of the relative humidity-dependent physical state of organic particulate matter in the uptake of semivolatile organic molecules. *Environ Sci Technol* 53:13209–13218. <https://doi.org/10.1021/acs.est.9b05354>
- He X, Leng C, Pang S, Zhang Y (2017a) Kinetics study of heterogeneous reactions of ozone with unsaturated fatty acid single droplets using micro-FTIR spectroscopy. *RSC Adv* 7:3204–3213. <https://doi.org/10.1039/C6RA25255A>
- He X, Pang S, Ma J, Zhang Y (2017b) Influence of relative humidity on heterogeneous reactions of O₃ and O₃/SO₂ with soot particles: potential for environmental and health effects. *Atmos Environ* 165:198–206. <https://doi.org/10.1016/j.atmosenv.2017.06.049>
- Jia L, Xu Y (2015) Ozone and secondary organic aerosol formation from ethylene–NO_x–NaCl irradiations under different relative humidity conditions. *J Atmos Chem* 73:81–100. <https://doi.org/10.1007/s10874-015-9317-1>
- Johnson CE, Stevenson DS, Collins WJ, Derwent RG (2001) Role of climate feedback on methane and ozone studied with a coupled ocean-atmosphere-chemistry model. *Geophys Res Lett* 28:1723–1726. <https://doi.org/10.1029/2000GL011996>
- Kavassalis SC, Murphy JG (2017) Understanding ozone-meteorology correlations: a role for dry deposition. *Geophys Res Lett* 44:2922–2931. <https://doi.org/10.1002/2016GL071791>
- Kotelnikov SN, Stepanov EV (2019) Role of aqueous aerosols in ozone decomposition in the near-surface atmosphere. *Bull Lebedev Phys Inst* 46:284–288. <https://doi.org/10.3103/S1068335619090045>
- Leu MT, Timonen RS, Keyser LF, Yung YL (1995) Heterogeneous reactions of HNO₃(g)+NaCl(s).fwdarw. HCl(g)+NaNO₃(s) and N₂O₅(g)+NaCl(s).fwdarw. ClNO₂(g)+NaNO₃(s). *J Phys Chem* 99:13203–13212. <https://doi.org/10.1021/j100035a026>
- Li R, Wang Z, Cui L et al (2019) Air pollution characteristics in China during 2015–2016: spatiotemporal variations and key meteorological factors. *Sci Total Environ* 648:902–915. <https://doi.org/10.1016/j.scitotenv.2018.08.181>
- Liu PF, Zhao CS, Göbel T et al (2011) Hygroscopic properties of aerosol particles at high relative humidity and their diurnal variations in the north China plain. *Atmos Chem Phys* 11:3479–3494. <https://doi.org/10.5194/acp-11-3479-2011>
- Lu X, Hong J, Zhang L et al (2018) Severe surface ozone pollution in China: a global perspective. *Environ Sci Technol Lett* 5:487–494. <https://doi.org/10.1021/acs.estlett.8b00366>
- Manju A, Kalaiselvi K, Dhanaanjan V et al (2018) Spatio-seasonal variation in ambient air pollutants and influence of meteorological factors in Coimbatore Southern India. *Air Qual Atmos Heal* 11:1179–1189. <https://doi.org/10.1007/s11869-018-0617-x>
- Monks PS, Archibald AT, Colette A et al (2015) Tropospheric ozone and its precursors from the urban to the global scale from air quality to short-lived climate forcer. *Atmos Chem Phys* 15:8889–8973
- Murazaki K, Hess P (2006) How does climate change contribute to surface ozone change over the United States? *J Geophys Res* 111:D05301. <https://doi.org/10.1029/2005JD005873>
- Olszyna KJ, Luria M, Meagher JF (1997) The correlation of temperature and rural ozone levels in southeastern U.S.A. *Atmos Environ* 31:3011–3022. [https://doi.org/10.1016/S1352-2310\(97\)00097-6](https://doi.org/10.1016/S1352-2310(97)00097-6)
- Ou J, Yuan Z, Zheng J et al (2016) Ambient ozone control in a photochemically active region: short-term despiking or long-term attainment? *Environ Sci Technol* 50:5720–5728. <https://doi.org/10.1021/acs.est.6b00345>
- Ou J, Zheng J, Li R et al (2015) Speciated OVOC and VOC emission inventories and their implications for reactivity-based ozone control strategy in the pearl river delta region, China. *Sci Total Environ* 530–531:393–402. <https://doi.org/10.1016/j.scitotenv.2015.05.062>
- Reddy PJ, Pfister GG (2016) Meteorological factors contributing to the interannual variability of midsummer surface ozone in Colorado, Utah, and other western U.S. states. *J Geophys Res* 121:2434–2456. <https://doi.org/10.1002/2015JD023840>
- Reichert L, Andrés Hernández MD, Stöbener D et al (2003) Investigation of the effect of water complexes in the determination of peroxy radical ambient concentrations: implications for the atmosphere. *J Geophys Res D Atmos*. <https://doi.org/10.1029/2002jd002152>
- Seinfeld JH, Pandis SN (2016) Atmospheric chemistry and physics: from air pollution to climate change, 2nd edn. Wiley, Hoboken, N.J.
- Shao M, Tang X, Zhang Y, Li W (2006) City clusters in China: air and surface water pollution. *Front Ecol Environ* 4:353–361. [https://doi.org/10.1890/1540-9295\(2006\)004\[0353:CCICAA\]2.0.CO;2](https://doi.org/10.1890/1540-9295(2006)004[0353:CCICAA]2.0.CO;2)
- Shao M, Zhang Y, Zeng L et al (2009) Ground-level ozone in the pearl river delta and the roles of VOC and NO_x in its production. *J Environ Manag* 90:512–518. <https://doi.org/10.1016/j.jenvman.2007.12.008>

- Tai APK, Mickley LJ, Jacob DJ (2010) Correlations between fine particulate matter (PM_{2.5}) and meteorological variables in the United States: implications for the sensitivity of PM_{2.5} to climate change. *Atmos Environ* 44:3976–3984. <https://doi.org/10.1016/j.atmosenv.2010.06.060>
- Thompson AM, Stewart RW, Owens MA, Herwehe JA (1989) Sensitivity of tropospheric oxidants to global chemical and climate change. *Atmos Res* 23:519–532. [https://doi.org/10.1016/0004-6981\(89\)90001-2](https://doi.org/10.1016/0004-6981(89)90001-2)
- Tu J, Xia ZG, Wang H, Li W (2007) Temporal variations in surface ozone and its precursors and meteorological effects at an urban site in China. *Atmos Res* 85:310–337. <https://doi.org/10.1016/j.atmosres.2007.02.003>
- Wang T, Nie W, Gao J et al (2010a) Air quality during the 2008 Beijing Olympics: secondary pollutants and regional impact. *Atmos Chem Phys* 10:7603–7615. <https://doi.org/10.5194/acp-10-7603-2010>
- Wang T, Xue L, Brimblecombe P et al (2017) Ozone pollution in China: a review of concentrations, meteorological influences, chemical precursors, and effects. *Sci Total Environ* 575:1582–1596. <https://doi.org/10.1016/j.scitotenv.2016.10.081>
- Wang X, Zhang Y, Hu Y et al (2010b) Process analysis and sensitivity study of regional ozone formation over the Pearl river delta, China, during the PRIDE-PRD2004 campaign using the community multiscale air quality modeling system. *Atmos Chem Phys* 10:4423–4437. <https://doi.org/10.5194/acp-10-4423-2010>
- Wang Y, Luo H, Jia L, Ge S (2016) Effect of particle water on ozone and secondary organic aerosol formation from benzene–NO₂–NaCl irradiations. *Atmos Environ* 140:386–394. <https://doi.org/10.1016/j.atmosenv.2016.06.022>
- Yang L, Luo H, Yuan Z et al (2019) Quantitative impacts of meteorology and precursor emission changes on the long-term trend of ambient ozone over the Pearl River Delta, China, and implications for ozone control strategy. *Atmos Chem Phys* 19:12901–12916. <https://doi.org/10.5194/acp-19-12901-2019>
- Yu S (2019) Fog geoengineering to abate local ozone pollution at ground level by enhancing air moisture. *Environ Chem Lett* 17:565–580. <https://doi.org/10.1007/s10311-018-0809-5>
- Yu S, Mathur R, Kang D et al (2006) Performance and diagnostic evaluation of ozone predictions by the eta-community multiscale air quality forecast system during the 2002 new England air quality study. *J Air Waste Manag Assoc* 56:1459–1471. <https://doi.org/10.1080/10473289.2006.10464554>
- Zanobetti A, Schwartz J (2008) Mortality displacement in the association of ozone with mortality: an analysis of 48 cities in the United States. *Am J Respir Crit Care Med* 177:184–189. <https://doi.org/10.1164/rccm.200706-823OC>
- Zhao B, Wang P, Ma JZ et al (2012) A high-resolution emission inventory of primary pollutants for the Huabei region, China. *Atmos Chem Phys* 12:481–501. <https://doi.org/10.5194/acp-12-481-2012>

P

Supplementary Information

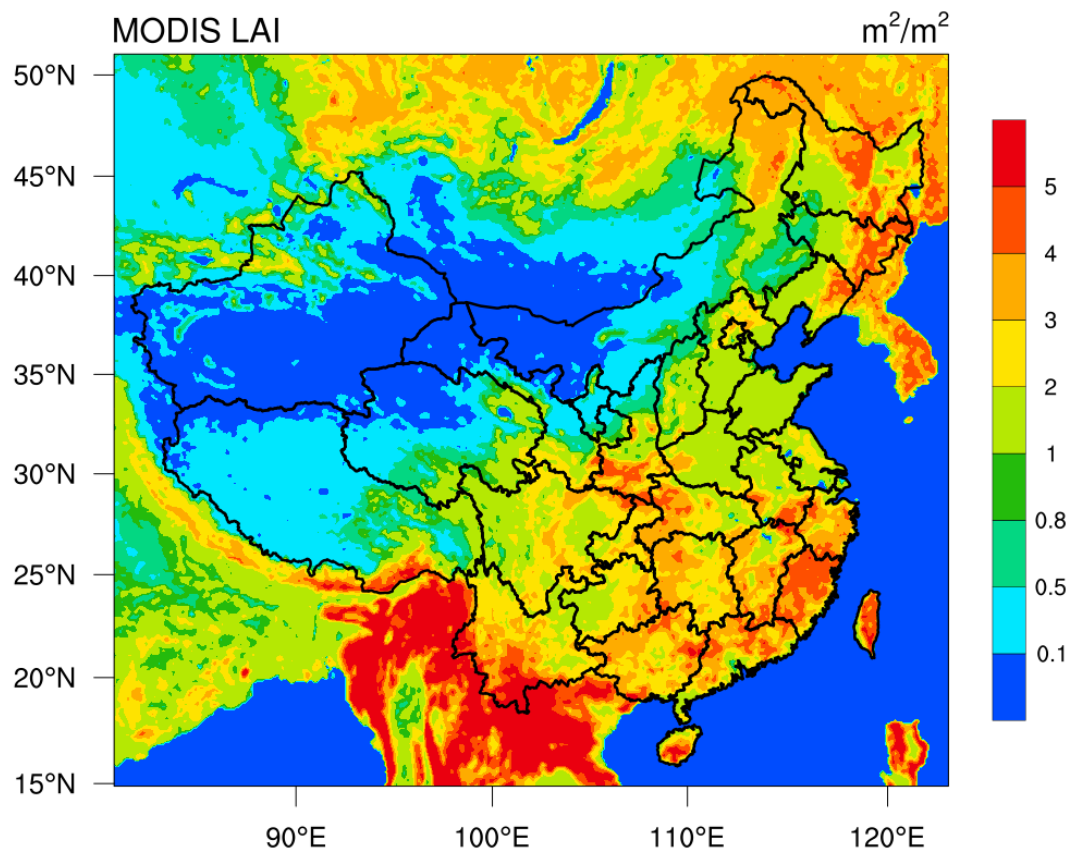


Fig. S1 Spatial distributions of leaf area indices (LAI) in summer season in China.

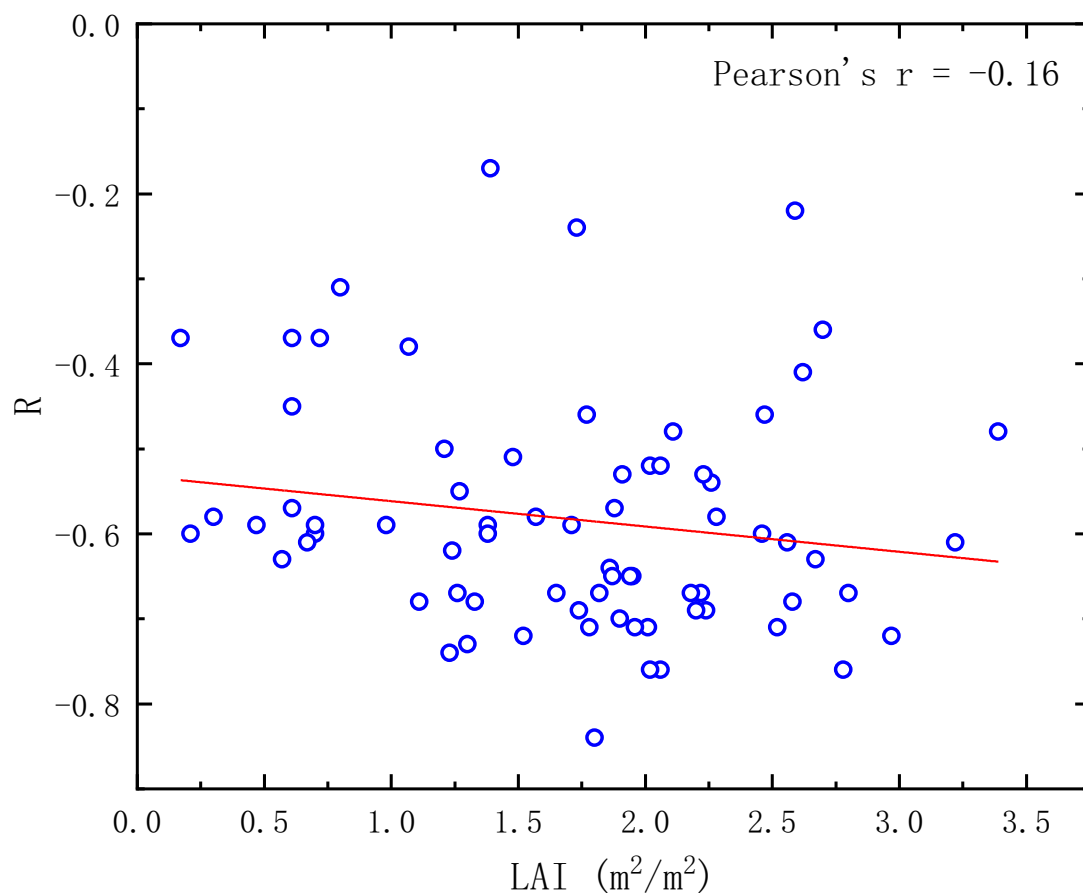


Fig. S2 Scatter plot and linear regression between leaf area indices (LAI) and correlation coefficients of O_3 and RH (R) across all the 74 cities.

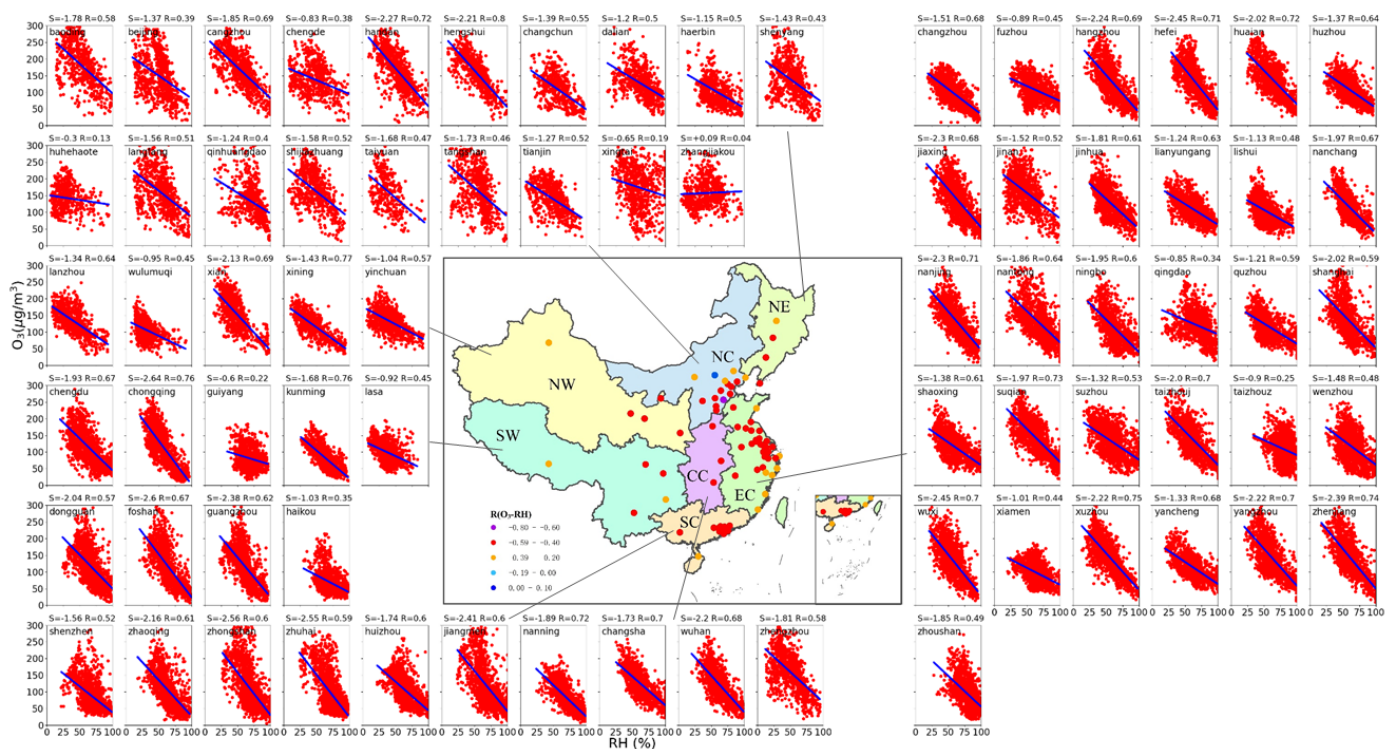


Fig. S3 Correlations between noontime O_3 and relative humidity (RH) (11:00 to 16:00, local time) by excluding data points

with precipitation and low T ($T \leq 15^\circ\text{C}$) in different warm seasons of 2017 and 2018 for the major 74 cities in China but for all RH values when compared to Fig. 2.

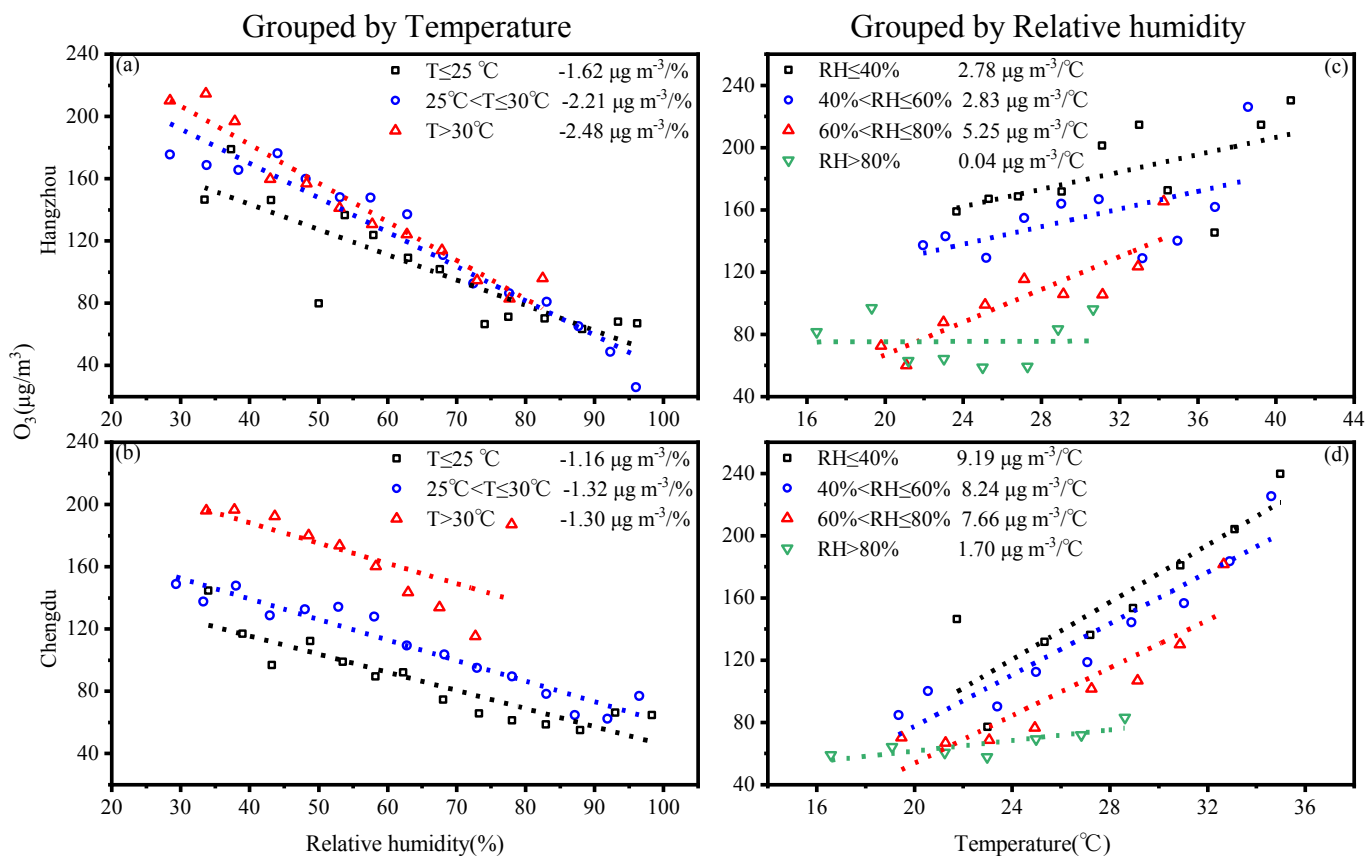


Fig. S4 Scatter plots of O_3 against relative humidity (RH) grouped by T during the noontime (11:00 to 16:00, local time) excluding precipitation in different warm seasons during 2017-2018 in (a) Hangzhou and (b) Chengdu. Points represent the average values of O_3 concentration versus RH for each RH bin (5% intervals). Scatter plots of O_3 against T grouped by RH during the same period as above in (c) Hangzhou and (d) Chengdu. Points represent the average values of O_3 concentrations versus T for each T bin (2°C intervals). The slopes of linear regression equations are also provided in the plots ($\alpha < 0.05$).

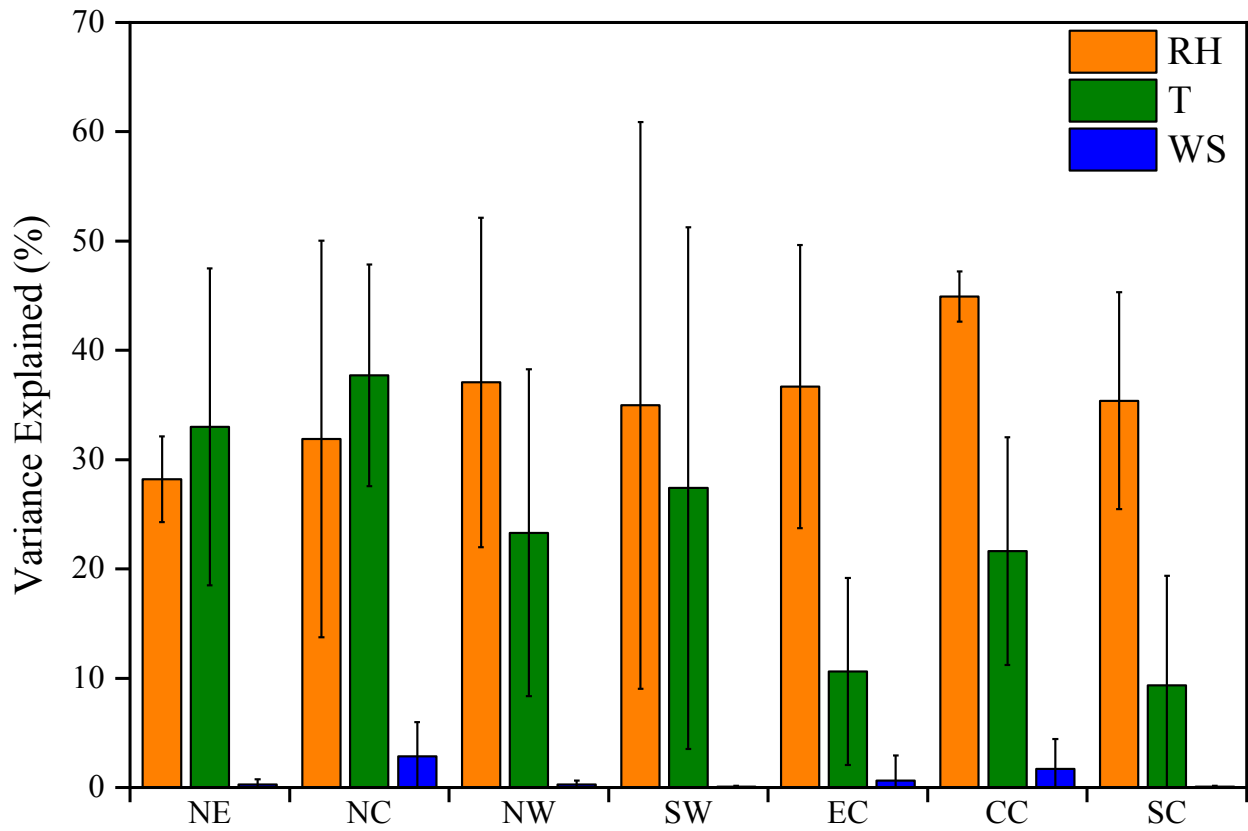


Fig. S5 Ozone variance attributed to meteorology conditions (relative humidity (RH), temperature (T), wind speed (WS)) during the noontime (11:00 to 16:00, local time) excluding precipitation in warm seasons in 2017-2018 averaged across all cities in seven regions. The variance explained is equal to the square of the correlation coefficient between O_3 and each factor multiplied by 100. The error bars represent standard deviation from the mean.

Table S1 Related water vapor-involved chemical reactions of O₃ formation (Yu, 2019).

O ₃ decomposition by water vapor	hydroxyl radicals termination reactions	NO ₂ termination reactions
$O_3 + hv \rightarrow O(^1D) + O_2$	$HO_2 + CO + nH_2O \rightarrow CO_2 + OH$	$O(^3P) + NO_2 + M \rightarrow NO_3 + M$
$O(^1D) + H_2O \rightarrow 2OH$	$HO_2 + NO + nH_2O \rightarrow \text{nonradical products}$	$NO_2 + O_3 \rightarrow NO_3 + O_2$
$O_3 + OH \rightarrow HO_2 + O_2$	$OH + CO + nH_2O \rightarrow \text{nonradical products}$	$NO_2 + NO_3 + M \rightarrow N_2O_5 + M$
$O_3 + HO_2 \rightarrow OH + 2O_2$		$2NO_2 + H_2O \rightarrow HONO + HNO_3$
		$N_2O_5 + H_2O \rightarrow 2HNO_3$
		$N_2O_{5(gas)} + NaCl \rightarrow ClNO_2 + NaNO_3$

Table S2 Average leaf area indices (LAI) in summer season, topography height (HGT_M) and at each of 74 major cities.

Region	City	LAI (m ² /m ²)	HGT_M (m)	R	Region	City	LAI (m ² /m ²)	HGT_M (m)	R
Northeast China	Dalian	0.61	28.34	-0.57	East China	Changzhou	1.65	10.08	-0.67
	Haerbin	2.11	160.38	-0.48		Fuzhou	2.62	146.11	-0.41
	Shenyang	2.26	93.31	-0.54		Hangzhou	1.74	40.92	-0.69
	Changchun	1.91	225.63	-0.53		Hefei	1.96	30.96	-0.71
North China	Baoding	1.95	9.38	-0.65		Huzhou	0.57	10.86	-0.63
	Beijing	1.77	99.48	-0.46		Huaian	2.24	10.05	-0.69
	Cangzhou	1.23	6.25	-0.74		Jinan	1.57	200.80	-0.58
	Chengde	2.70	573.66	-0.36		Jiaxing	2.22	7.02	-0.67
	Handan	2.01	42.66	-0.71		Jinhua	2.56	166.92	-0.61
	Hengshui	1.80	16.84	-0.84		Lishui	3.39	423.98	-0.48
	Huhehaote	1.07	1243.88	-0.38		Lianyungang	0.70	22.56	-0.6
	Langfang	1.71	8.34	-0.59		Nanchang	1.82	18.14	-0.67
	Qinhuangdao	0.17	19.13	-0.37		Nanjing	1.78	32.89	-0.71
	Shijiazhuang	1.94	55.65	-0.65		Nantong	2.28	3.60	-0.58
	Taiyuan	1.27	1059.15	-0.55		Ningbo	0.98	30.16	-0.59
	Tangshan	1.48	51.95	-0.51		Qingdao	0.72	80.12	-0.37
	Tianjin	1.38	5.08	-0.59		Quzhou	2.06	94.15	-0.52
	Xingtai	2.02	43.76	-0.52		Xiamen	0.61	58.70	-0.45
Zhangjiakou	1.39	1221.46	-0.17	Shanghai		0.21	2.58	-0.6	
South China	Dongguan	1.88	54.88	-0.57		Shaoxing	1.38	17.28	-0.6
	Foshan	1.26	16.69	-0.67	Suzhou	1.21	7.51	-0.5	
	Guangzhou	2.67	104.44	-0.63	Taizhouz	1.73	41.10	-0.24	
	Haikou	0.00	1.70	-0.35	Taizhouj	2.80	17.88	-0.67	
	Huizhou	2.46	91.05	-0.6	Wenzhou	2.47	123.08	-0.46	
	Jiangmen	0.67	10.09	-0.61	Wuxi	1.90	9.70	-0.7	
	Nanning	2.97	146.45	-0.72	Suqian	2.52	14.67	-0.71	
	Shenzhen	2.23	78.31	-0.53	Xuzhou	2.06	42.81	-0.76	
	Zhaoqing	3.22	133.32	-0.61	Yancheng	1.86	3.23	-0.64	
	Zhongshan	0.70	8.05	-0.59	Yangzhou	2.20	2.27	-0.69	
	Zhuhai	0.47	16.43	-0.59	Zhenjiang	1.52	5.10	-0.72	
Northwest China	Lanzhou	0.30	1802.68	-0.58	Zhoushan	0.00	8.10	-0.49	
	Wulumuqi	0.61	754.52	-0.37	Southwest China	Chengdu	2.18	591.93	-0.67
	Xian	1.33	456.64	-0.68		Guiyang	2.59	1240.98	-0.22
	Xining	1.30	2569.29	-0.73		Kunming	2.78	2100.75	-0.76
Yinchuan	1.24	1138.26	-0.62	Chongqing		2.02	356.03	-0.76	
Central China	Wuhan	1.11	21.65	-0.68		Lasa	0.80	4387.26	-0.31
	Changsha	2.58	65.72	-0.68					
	Zhengzhou	1.87	90.75	-0.65					

Table S3 Statistical values of O₃ concentrations under RH_≥75% and RH under O₃≥200 μg m⁻³. Min, Max, Mean, SD, 90% denotes the minimum, maximum, mean, standard deviation, and 90% percentile of corresponding parameters, respectively. NaN represents no values, that is, no O₃ concentrations exceeds 200 μg m⁻³ for these cities. The average O₃ concentrations varied in the range of 44.6 and 122.5 μg m⁻³ with 90% percentile of hourly O₃ values ranging from 75.6 to 168.7 μg m⁻³ in all the 74 cities under RH over 75%, lower than China National Ambient Air Quality Standard (CNAAQs, GB3095-2012, 200 μg m⁻³), showing the important role of high RH in O₃ attainment in warm seasons at all cities.

Region	City	O ₃ (μg m ⁻³) under RH _≥ 75%			RH (%) under O ₃ ≥200 μg m ⁻³		
		[Min, Max]	Mean ± SD	90%	[Min, Max]	Mean ± SD	90%
Northeast China	Dalian	[32.9, 190.8]	93.5 ± 29.3	131.9	[29, 70]	47 ± 11	66
	Haerbin	[29.2, 157.4]	70.7 ± 31.5	109.5	[27, 54]	43 ± 10	52
	Shenyang	[15.5, 126.1]	59.0 ± 31.9	99.3	[26, 69]	43 ± 10	56
	Changchun	[20.6, 151.5]	58.9 ± 21.7	79.4	[28, 59]	45 ± 10	57
North China	Baoding	[36.6, 199.7]	110.8 ± 38.1	157.2	[26, 71]	44 ± 11	58
	Beijing	[16.2, 131.5]	70.5 ± 28.7	111.2	[26, 63]	46 ± 10	57
	Cangzhou	[26.7, 189.0]	95.1 ± 34.5	136.9	[26, 73]	42 ± 11	58
	Chengde	[15.2, 163.0]	88.1 ± 34.2	128.9	[27, 62]	42 ± 9	54
	Handan	[31.5, 167.3]	91.1 ± 30.0	125.9	[26, 68]	40 ± 10	54
	Hengshui	[19.3, 133.3]	80.3 ± 27.7	110.9	[26, 67]	38 ± 8	47
	Huhehaote	[61.8, 159.9]	101.2 ± 33.0	149.0	[26, 39]	32 ± 4	36
	Langfang	[26.3, 172]	82.7 ± 35.6	125.2	[27, 73]	46 ± 11	60
	Qinhuangdao	[16.6, 302.2]	110.7 ± 43.4	162.1	[28, 82]	63 ± 14	78
	Shijiazhuang	[13.5, 174.1]	85.5 ± 37.4	136.8	[26, 70]	40 ± 10	52
	Taiyuan	[80.3, 134.5]	103.4 ± 20.7	123.3	[26, 49]	34 ± 6	43
	Tangshan	[13.0, 211.2]	90.3 ± 51.8	168.7	[27, 76]	48 ± 13	65
	Tianjin	[27.1, 185.4]	77.0 ± 31.4	99.7	[26, 62]	39 ± 7	47
	Xingtai	[15.8, 226.0]	98.0 ± 51	165.1	[27, 78]	46 ± 13	63
Zhangjiakou	[77.8, 182.8]	122.5 ± 25.9	155.4	[26, 71]	45 ± 9	58	
Northwest China	Lanzhou	[37.0, 107.2]	75.7 ± 22.4	105.7	[26, 52]	39 ± 8	46
	Wulumuqi	[39.7, 107.1]	67.0 ± 22.3	90.5	NaN		
	Xian	[34.7, 124.6]	76.5 ± 23.0	109.9	[26, 54]	36 ± 7	47
	Xining	[34.8, 108.0]	64.8 ± 16.8	85.9	NaN		
	Yinchuan	[49.3, 110.9]	82.6 ± 14.6	99.3	[26, 38]	31 ± 4	37
Southwest China	Chengdu	[15.8, 187.2]	69.2 ± 25.8	103.6	[32, 69]	46 ± 9	58
	Guiyang	[23.6, 160.7]	76.2 ± 27.9	114.9	NaN		
	Kunming	[13.7, 115.1]	53.5 ± 19.6	81.1	NaN		
	Chongqing	[10.9, 151.1]	44.6 ± 23.0	75.6	[28, 55]	41 ± 7	50
	Lasa	NaN			NaN		
East China	Changzhou	[10.6, 125.9]	53.1 ± 24.0	88.5	NaN		
	Fuzhou	[26.4, 180]	91.2 ± 26.6	128.2	NaN		
	Hangzhou	[18.4, 148.7]	70.7 ± 28.1	113.9	[27, 71]	44 ± 9	54
	Hefei	[20.9, 168.6]	76.2 ± 28.4	116.1	[31, 68]	52 ± 8	62
	Huzhou	[31.6, 188.2]	70.6 ± 24.1	98.0	[39, 49]	43 ± 5	47
	Huaian	[27.8, 189.0]	94.4 ± 32.1	134.7	[26, 67]	43 ± 10	57
	Jinan	[10.9, 222.9]	79.9 ± 43.8	129.2	[26, 84]	42 ± 11	55
	Jiaxing	[22.7, 216.0]	86.0 ± 35.6	136.8	[27, 75]	50 ± 10	64
	Jinhua	[15.7, 144.0]	78.8 ± 28.4	114.1	[28, 70]	42 ± 9	55

	Lishui	[24.7, 134.0]	73.1 ± 21.4	103.0	[30, 49]	40 ± 7	46
	Lianyungang	[29.4, 160.0]	80.0 ± 22.8	109.2	[34, 44]	38 ± 4	42
	Nanchang	[21.6, 177.4]	73.1 ± 26.9	103.7	[33, 50]	40 ± 6	49
	Nanjing	[9.7, 187.2]	80.8 ± 34.4	126.0	[28, 67]	47 ± 9	58
	Nantong	[24.8, 308.0]	94.7 ± 38.0	142.0	[26, 93]	50 ± 12	69
	Ningbo	[22.3, 200.6]	78.7 ± 30.9	115.6	[29, 90]	47 ± 10	59
	Qingdao	[14.3, 241.2]	99.9 ± 39.5	151.7	[43, 89]	58 ± 11	73
	Quzhou	[31.0, 155.0]	88.5 ± 27.1	128.9	[28, 47]	37 ± 5	43
	Xiamen	[32.5, 170.7]	75.8 ± 23.7	106.3	NaN		
	Shanghai	[24.5, 302.1]	84.9 ± 41	139.2	[26, 91]	47 ± 10	58
	Shaoxing	[35.0, 172.5]	83.0 ± 23.9	115.6	[28, 49]	38 ± 6	45
	Suzhou	[31.7, 233.4]	97.4 ± 37.9	153.0	[26, 77]	45 ± 14	68
	Taizhouz	[18.0, 231.7]	103.1 ± 37.7	151.3	[50, 92]	66 ± 12	81
	Taizhouj	[33.0, 227.3]	90.0 ± 32	125.7	[26, 81]	44 ± 12	58
	Wenzhou	[20.3, 208]	80.3 ± 37.3	136.1	[31, 75]	51 ± 8	60
	Wuxi	[14.4, 187.9]	64.0 ± 30.5	100.9	[26, 67]	42 ± 9	54
	Suqian	[19.8, 191]	93.0 ± 33.5	138.0	[26, 71]	44 ± 9	57
	Xuzhou	[16.8, 175.4]	71.5 ± 26.0	101.7	[26, 67]	40 ± 8	50
	Yancheng	[35.0, 155.5]	83.5 ± 20.5	107.8	[27, 52]	37 ± 7	48
	Yangzhou	[13.0, 212.4]	87.5 ± 30.1	126.5	[26, 76]	46 ± 10	58
	Zhenjiang	[9.3, 193.3]	83.1 ± 34.1	132.6	[26, 69]	46 ± 10	60
	Zhoushan	[17.3, 221.3]	81.1 ± 37.3	132.2	[49, 80]	64 ± 9	74
Central China	Wuhan	[21.8, 152.3]	68.9 ± 25.7	102.9	[30, 66]	46 ± 7	53
	Changsha	[22.7, 163.6]	81.7 ± 26	117.8	[27, 65]	42 ± 8	52
	Zhengzhou	[26.6, 149.1]	79.3 ± 27.3	107.4	[26, 66]	39 ± 9	54
South China	Dongguan	[9.8, 228.2]	72.1 ± 38.1	119.6	[42, 85]	57 ± 8	70
	Foshan	[7.4, 212.0]	58.6 ± 30.9	93.2	[28, 84]	52 ± 9	61
	Guangzhou	[13.3, 181.7]	60.7 ± 35.3	114.4	[40, 67]	52 ± 6	60
	Haikou	[20.2, 131.4]	56.7 ± 22.8	89.2	[51, 68]	62 ± 6	67
	Huizhou	[23.0, 219.8]	70.5 ± 32.8	114.6	[46, 95]	60 ± 11	69
	Jiangmen	[9.0, 288.3]	73.1 ± 38	114.0	[28, 93]	53 ± 12	66
	Nanning	[8.0, 139.0]	53.8 ± 23.5	85.1	[59, 61]	60 ± 1	61
	Shenzhen	[27.7, 208.5]	67.9 ± 31.8	110.3	[38, 84]	57 ± 11	71
	Zhaoqing	[16.0, 231.3]	64.8 ± 41.4	123.3	[37, 87]	53 ± 10	64
	Zhongshan	[6.0, 270.3]	70.6 ± 34.7	112.1	[30, 76]	52 ± 10	66
	Zhuhai	[16.8, 250.3]	70.4 ± 35.4	110.8	[26, 81]	55 ± 14	73